Erdem Acar[1]
Ph.D.
e-mail: eacar@ufl.edu

Raphael T. Haftka
Distinguished Professor
e-mail: haftka@ufl.edu

Mechnical and Aerospace Engineering Department,
University of Florida,
Gainesville, FL 32611

Theodore F. Johnson
Ph.D. Aerospace Engineer
NASA Langley Research Center,
Hampton, VA 23681
e-mail: theodore.f.johnson@nasa.gov

Tradeoff of Uncertainty Reduction Mechanisms for Reducing Weight of Composite Laminates

Inspired by work on allocating risk between the different components of a system for a minimal cost, we explore the optimal allocation of uncertainty in a single component. The tradeoffs of uncertainty reduction measures on the weight of structures designed for reliability are explored. The uncertainties in the problem are broadly classified as error and variability. Probabilistic design is carried out to analyze the effect of reducing error and variability on the weight. As a demonstration problem, the design of composite laminates at cryogenic temperatures is chosen because the design is sensitive to uncertainties. For illustration, variability reduction takes the form of quality control, while error is reduced by including the effect of chemical shrinkage in the analysis. Tradeoff plots of uncertainty reduction measures, probability of failure and weight are generated that could allow choice of optimal uncertainty control measure combination to reach a target probability of failure with minimum cost. In addition, the paper also compares response surface approximations to direct approximation of a probability distribution for efficient estimation of reliability. [DOI: 10.1115/1.2406097]

1 Introduction

For systems composed of multiple components, system failure probability depends on the failure probabilities of the components, and the cost of changing the failure probability may vary from one component to another. The risk or reliability allocation problem can be defined [1–3] as determining the optimal component reliabilities such that the system objective function (e.g., cost) is optimized and all design constraints (e.g., system reliability level) are met. Several researchers applied risk and reliability allocation methods to optimize the total cost of nuclear power plants by allocating the risk and reliability of individual subsystems such that a specified reliability goal is met [4–7]. Ivanovic [8] applied reliability allocation to design of a motor vehicle. The vehicle reliability is allocated to its elements for minimum vehicle cost while keeping the reliability of the vehicle at a specified level. Acar and Haftka [9] investigated reliability allocation between the wing and tail of a transport aircraft. The concept of risk allocation is also used in finance applications, where risk allocation is defined as the process of apportioning individual risks relating to projects and service delivery to the party best placed to manage each risk. Risks are allocated across the supply chain—that is, between the department, its customers, its suppliers and their subcontractors. Refs. [10–12] are some examples of numerous publications on risk allocation in finance applications.

Instead of considering a system of multiple components, we may also consider multiple sources of uncertainty for a single component. Again, the probability of failure can be reduced by reducing the uncertainty from each source, with different cost associated with each. That is, the probability constraints can be satisfied by reducing different types of uncertainties. The objective of this paper is to demonstrate this approach for reliability based design optimization (RBDO) of structures.

Over the years, researchers have proposed different classifications for uncertainty. Oberkampf et al. [13,14] provided an analysis of uncertainty in engineering modeling and simulations. Here as in our previous work (Acar et al. [15,16]), we use a simplified uncertainty classification. Uncertainty is divided into error and variability, to distinguish between uncertainties that apply equally to an entire fleet of a structural model (error) and the uncertainties that vary for an individual structure (variability).

In aircraft structural design there are different players engaged in uncertainty reduction. Researchers reduce errors by developing better models of failure prediction and this leads to safer structures (Acar et al. [17]). Aircraft companies constantly improve finite element models, thus reducing errors in structural response. The Federal Aviation Administration (FAA) leads to further reduction in error (Ref. [15]) through the process of certification testing. Aircraft makers also constantly improve manufacturing techniques and quality control procedure to reduce variability between airplanes. Airlines reduce variability in structural failure due to operating conditions by conducting inspections, and the FAA contributes to reduced variability by licensing pilots, thereby reducing the risk that incompetent pilots may subject airplanes to excessively high loads.

These uncertainty reduction mechanisms are costly, and their cost can be traded against the cost of making the structure safer by increasing its weight. Kale et al. [18] investigated the tradeoff of inspection cost against the cost of structural weight, and found that inspections are quite cost effective. Qu et al. [19] analyzed the effect of variability reduction on the weight savings from composite laminates under cryogenic conditions. They found that employing quality control to -2σ for the transverse failure strain may reduce the weight of composite laminates operating at cryogenic temperatures by 25% marking such laminates as a structure where weight is sensitive to the magnitude of uncertainties.

In this paper, we use the example of this composite laminate to explore tradeoffs between the variability reduction, considered by Qu et al. [19], and error reduction in the form of improved accuracy of structural analysis.

The paper is structured as follows. Section 2 discusses the design of composite laminates for cryogenic temperatures. Probability of failure estimation of the laminates is described in Sec. 3. The probabilistic design optimization problem is discussed in Sec. 4. Weight savings using error and variability reduction mecha-

[1]Corresponding author. Currently Post-doctoral research associate at the Center for Advanced Vehicular Systems, Mississippi State University, Mississippi State, MS 39579.

Contributed by the Design Automation Committee of ASME for publication in the JOURNAL OF MECHANICAL DESIGN. Manuscript received September 19, 2005; final manuscript received February 23, 2006. Review conducted by Shapour Azarm. Paper presented at the ASME 2005 Design Engineering Technical Conferences and Computers and Information in Engineering Conference (DETC2005), September 24–28, 2005, Long Beach, California, USA.

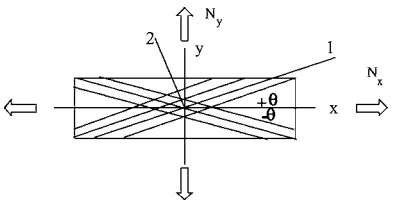

Fig. 1 Geometry and loading of the laminate with two ply angles $[\pm\theta_1/\pm\theta_2]_s$ (*x*-is the hoop direction and *y* is the axial direction)

nisms are given in Sec. 5. The optimum use of uncertainty reduction mechanisms are discussed in Sec. 6, followed by concluding remarks in Sec. 7.

2 Design of Composite Laminates for Cryogenic Temperatures

We consider the design of a composite panel at cryogenic temperatures as demonstration for trading off uncertainty reduction mechanisms. The definition of the problem is taken directly from Qu et al. [19]. The laminate (Fig. 1) is subject to mechanical loading (N_x is 4800 lb./in. and N_y is 2400 lb./in.) and thermal loading due to the operating temperature −423°F, where the stress-free temperature is 300°F.

The objective is to optimize the weight of laminates with two ply angles $[\pm\theta_1/\pm\theta_2]_s$. The design variables are the ply angles θ_1, θ_2 and ply thicknesses t_1, t_2. The material used in the laminates is IM600/133 graphite–epoxy of ply thickness 0.005 in. The minimum thickness necessary to prevent hydrogen leakage is assumed to be 0.04 in. The geometry and loading conditions are shown in Fig. 1. Temperature-dependent material properties are given in Appendix A.

The deterministic design optimization of the problem was solved by Qu et al. [19]. They used continuous design variables and rounded the thicknesses to integer multiples of the basic ply thickness 0.005 in. In the deterministic optimization, they multiplied the strains by a safety factor of $S_F=1.4$.

The deterministic optimization problem is formulated as

$$\min h = 4(t_1 + t_2)$$

$$\text{s.t.} \quad \varepsilon_1^L \leq S_F\varepsilon_1 \leq \varepsilon_1^U, \varepsilon_2^L \leq S_F\varepsilon_2 \leq \varepsilon_2^U, S_F|\gamma_{12}| \leq \gamma_{12}$$

$$t_1, t_2 \geq 0.005 \tag{1}$$

where the allowable strains are given in Table 1.

Since designs must be feasible for the entire range of temperatures, strain constraints were applied at 21 different temperatures, which were uniformly distributed from 77°F to −423°F. Qu et al. [19] found the optimum design given in Table 2.

3 Calculation of the Probability of Failure

The failure of the laminates is assessed based on the first ply failure according to the maximum strain failure criterion. The strain allowables listed in Table 1 are the mean values of the failure strains according to Qu et al. [19].

Table 1 Allowable strains for IM600/133

ε_1^L	ε_1^U	ε_2^L	ε_2^U	γ_{12}^U
−0.0109	0.0103	−0.013	0.0154	0.0138

Table 2 Deterministic optimum design by Qu et al. [19]. The number in parentheses denote the unrounded design thickness

θ_1 (deg)	θ_2 (deg)	t_1 (in)	t_2 (in)	h (in)
27.04	27.04	0.010	0.015	0.100(0.095)

The first step in the calculation of the probability of failure is to quantify uncertainties included in the problem. As we discussed earlier, we use a simple classification for uncertainty that we used in our previous work (Acar et al. [15,16]). Uncertainty is divided into two parts, error and variability, to distinguish between the uncertainties that apply equally to the entire fleet of a structural model (error) and the uncertainties that vary for an individual structure (variability). Since errors are epistemic, they are often modeled using fuzzy numbers or possibility analysis (Refs. [20–22]). We model the errors probabilistically by using uniform distributions to maximize the entropy.

Variability refers to the departure of a quantity in individual laminates that have the same design. Here, the elastic properties (E_1, E_2, G_{12}, and ν_{12}), coefficients of thermal expansion (α_1 and α_2), failure strains (ε_1^L, ε_1^U, ε_2^L, ε_2^U, and γ_{12}^U) and the stress-free temperature (T_{zero}) have variability. These random variables are all assumed to follow uncorrelated normal distributions, with coefficients of variations listed in Table 3.

We also use a simple error model, assuming that calculated values of failure strains differ from actual values due to experimental or measurement errors. Using standard classical lamination theory (CLT) for ply strain calculation leads to errors in part, because standard CLT does not take chemical shrinkage into account. We relate the actual values of the strains to their calculated values via Eq. (2)

$$\varepsilon_{\text{calc}} = (1 + e)\varepsilon_{\text{true}} \tag{2}$$

where e is the representative error factor that includes the effect of all error sources on the values of strains and failure strains. For example, if the estimated failure strain is 10% too high, this is approximately equivalent to the strain being calculated 10% too low. For the error factor e, we use a uniform distribution with bounds of $\pm b_e$. This error bound can be reduced by using more accurate failure models. For example, the cure reference method [23] may be used to account for the shrinkage due to a chemical process. In Secs. 4 and 5, we will investigate the effect of reducing b_e on the probability of failure and the weight.

To calculate the probability of failure, we use Monte Carlo Simulation (MCS). For acceptable accuracy, sufficient strain analyses (simulations) must be obtained through standard CLT analysis. However, this is computationally expensive and needs to be repeated many times during the optimization. In order to reduce the computational cost, Qu et al. [19] used response surface approximations for strains (ε_1 in θ_1, ε_1 in θ_2, ε_2 in θ_1, ε_2 in θ_2, γ_{12} in θ_1, and γ_{12} in θ_2). They fitted quadratic response surface approximations to strains in terms of four design variables (t_1, t_2, θ_1, and θ_2), material parameters (E_1, E_2, G_{12}, ν_{12}, α_1, and α_2) and service temperature T_{serv}. These response surfaces were called the analysis response surfaces (ARS), because they replace the CLT analysis. A quadratic response surface approximation in terms of 12 variables includes 91 coefficients, so they used 182 realizations

Table 3 Coefficients of variation of the random variables (assumed uncorrelated normal distributions)

E_1, E_2, G_{12}, and ν_{12}	α_1 and α_2	T_{zero}	ε_1^L and ε_1^U	ε_2^L, ε_2^U, and γ_{12}^U
0.035	0.035	0.03	0.06	0.09

Table 4 Evaluation of the accuracy of the analysis response surface (ARS) used by Qu et al. [19]. Note that the strains are in millistrains.

	ε_1 in θ_1	ε_1 in θ_2	ε_2 in θ_1	ε_2 in θ_2	γ_{12} in θ_1	γ_{12} in θ_2
R^2_{adj} [a]	0.9977	0.9978	0.9956	0.9961	0.9991	0.9990
RMSE Predictor[b]	0.017	0.017	0.060	0.055	0.055	0.060
Mean of response	1.114	1.108	8.322	8.328	−3.13	−3.14

[a]Adjusted coefficient of multiple determination.
[b]Root mean square error predictor.

from Latin hypercube sampling (LHS) design. As seen from Table 4 the root mean square error predictions are less than 2% of the mean responses, so the accuracies of the ARS is good.

We found, however, that even small errors in strain values may lead to large errors in probability of failure calculations, so we considered approximate cumulative distribution functions (CDF) of strains instead of ARS. We assume normal distributions for strains and estimate the mean and the standard deviation of strains conservatively by MCS. That is, the mean and standard deviation of the assumed distribution are found so that the CDF of the approximated distribution is smaller than or equal to (i.e., more conservative) the CDF calculated via MCS, except for strain values very near the tail of the distribution. Detailed information on conservative CDF fitting is given in Appendix B. We use 1000 MCS simulations, which are accurate to a few percent of the standard deviation for estimating the mean and standard deviation. Cumulative distribution function obtained through 1000 MCS, the approximate normal distribution and the conservative approximate normal distributions for ε_2 corresponding to the deterministic optimum given in Table 2 are compared in Figs. 2(*a*) and 2(*b*).

Next, we compare the accuracy of the analysis response surface and approximate CDF approaches by using 1,000,000 MCS in Table 5. We can see that the use of approximate CDFs for strains leads to more accurate probability of failure estimations than the use of ARS. Furthermore, the case of conservative fit to CDF leads to overestimation of the probability of failure. However, the approximate CDFs were obtained by performing 1000 MCS, while the ARS were constrained by using only 182 MCS. In addition, the approximate CDF needs to be repeatedly calculated for each design. It is possible that some combination of ARS with approximate CDF may be more efficient and accurate than either using ARS or approximate CDF alone, and this will be explored in future work.

4 Probabilistic Design Optimization

The laminates are designed for a target failure probability of 10^{-4}. The optimization problem can be formulated as given in Eq. (3). The design variables are the ply thicknesses and angles

$$\min h = 4(t_1 + t_2)$$

$$\text{s.t.} \quad P_f \leqslant (P_f)_{\text{target}}$$

$$t_1, t_2 \geqslant 0.005 \tag{3}$$

For this optimization, we need to fit a design response surface (DRS)[2] to the probability of failure in terms of the design variables. The accuracy of the DRS may be improved by using an inverse safety measure. We use the probabilistic sufficiency factor (PSF) developed by Qu and Haftka [24].

4.1 Probabilistic Sufficiency Factor (PSF). The safety factor S is defined as the ratio of the capacity G_C of the structure to the structural response G_R. The PSF is the probabilistic interpretation of the safety factor S with its CDF defined as

[2]The term design response surface (DRS) follows Qu et al. [19] and indicates approximations to the probability of failure or other measures of safety as a function of design variables.

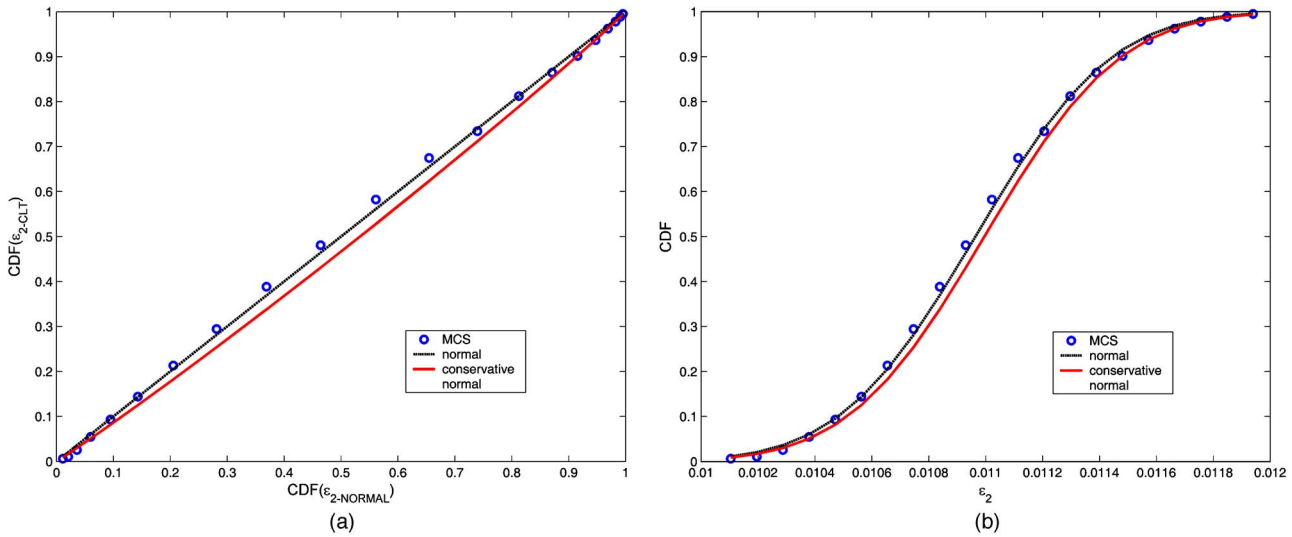

Fig. 2 Comparison of CDF obtained via 1000 MCS, the approximate normal distribution and conservative approximate normal distributions for ε_2 on θ_1 corresponding to the deterministic optimum: (*a*) CDF versus strain, (*b*) actual (empirical) CDF versus fitted CDF

Table 5 Comparison of probability of failure estimations for the deterministic optimum of Qu et al. [19]. Samples size of MCS is 1,000,000.

Approach followed	Probability of failure, P_f ($\times 10^{-4}$)	Standard error in P_f due to limited sampling ($\times 10^{-4}$)
MCS with CLT (exact analysis)	10.21	0.320
MCS with ARS[a] of strains	16.83	0.410
MCS with approximation to CDF of strains	11.55	0.340

[a]ARS=analysis response surface approximation.

$$F_S(s) = \text{Prob}\left(\frac{G_C}{G_R} \leqslant s\right) \tag{4}$$

Given a target probability of failure, $(P_f)_{\text{target}}$, PSF is defined as the solution to

$$F_S(s) = \text{Prob}\left(\frac{G_C}{G_R} \leqslant \text{PSF}\right) = \text{Prob}(S \leqslant \text{PSF}) = (P_f)_{\text{target}} \tag{5}$$

That is, the PSF is the safety factor obtained by equating the CDF of the safety factor to the target failure probability. The PSF takes values such that

$$\text{PSF} = \begin{cases} <1 & \text{if } P_f > (P_f)_{\text{target}} \\ =1 & \text{if } P_f = (P_f)_{\text{target}} \\ >1 & \text{if } P_f < (P_f)_{\text{target}} \end{cases} \tag{6}$$

When MCS are used, the PSF can be estimated as the nth smallest safety factor over all MCS, where $n = N \times (P_f)_{\text{target}}$. Using the PSF, the optimization problem can be formulated as

$$\min h = 4(t_1 + t_2)$$

$$\text{s.t.} \quad \text{PSF} \geqslant 1$$

$$t_1, t_2 \geqslant 0.005 \tag{7}$$

The optimization problem given in Eq. (7) is solved by using sequential quadratic programming (SQP) using function *fmincon* in MATLAB.

4.2 Design Response Surface (DRS). We have three components of strain for each angle: ε_1, ε_2, and γ_{12}. The strain ε_2 and γ_{12} are more critical than ε_1. The mean and standard deviation of four strains (ε_2 in θ_1, ε_2 in θ_2, γ_{12} in θ_1, and γ_{12} in θ_2) are computed by using MCS of sample size 1,000 and fitted with conservative normal distributions as shown in Fig. 2. The correlations between these distributions were low, and so the strains were treated as independent in MCS using 1,000,000 simulations at each design point to compute PSF. In order to perform the optimization, we need to approximate the PSF in terms of the design variables by a DRS. We fit three DRS of the PSF as function of the four design variables (t_1, t_2, θ_1, and θ_2) for three different error bound (b_e) values of 0, 10%, and 20%. As shown in Appendix C, the use of the PSF leads to much more accurate estimate of the safety margin than fitting a DRS to the probability of failure.

5 Weight Savings by Reducing Error and Quality Control

As noted earlier, the probabilistic design optimizations of the composite laminates were performed for three different values of the error bound, b_e, namely 0, 10%, and 20%. Schultz et al. [25] have shown that neglecting chemical shrinkage leads to substantial errors in strain calculations. Based on Ref. [25], we assume that using the standard CLT without chemical shrinkage leads to 20% errors in strain calculations, while using the modified CLT (i.e., CLT that takes chemical shrinkage into account) leads to the reduction of error bounds from 20% to 10%. As noted earlier, the errors are assumed to have uniform distribution, which corresponds to maximum entropy.

Table 6 Probabilistic optimum designs for different error bounds when only error reduction is applied. The PSF and P_f given in the last two columns are calculated via Monte Carlo simulations (sample size of 10,000,000) where the strains are directly computed via standard CLT analysis. The numbers in parentheses under PSF and P_f show the standard errors due to limited Monte Carlo sampling.

Error bound	θ_1 θ_2 (deg)	t_1 t_2 (in.)	h (in.) $[\Delta h(\%)]$[a]	PSF	P_f (1×10^{-4})
0	25.47	0.0156	0.1169	0.9986	1.017
	26.06	0.0137	[23.1]	(0.0030)	(0.032)
10%	25.59	0.0167	0.1332	1.018	0.598
	25.53	0.0167	[12.4]	(0.0035)	(0.024)
20%	23.71	0.0189	0.1520	0.9962	1.111
	23.36	0.0191	[0.0]	(0.0035)	(0.105)

[a]The optimum laminate thickness for 20% error bound is taken as the basis for Δh computations.

For the error bounds discussed, we solve the optimization problem given in Eq. (7). The results of the optimization are presented in Table 6 and the weight (proportional to thickness) savings due to error reduction are shown in Fig. 3. We see that reducing the error bounds from 20% to 10% leads to 12.4% weight saving. In addition, reducing error from 20% to 0 (clearly only a hypothetical case) leads to weight saving of 23.1%.

We have shown that it is possible to reduce the laminate thickness by 12.4% through reducing the error from 20% to 10%. Now, we combine error reduction with variability reduction and analyze the overall benefit of both uncertainty reduction mechanisms. An example of variability reduction is testing a set of composite laminates and rejecting the laminates having lower failure strains as a form of quality control. The test can involve a destructive evaluation of a small coupon cut out from laminate used to build the structure. Alternatively, it can involve a nondestructive scan of laminates to detect flaws known to be associated with lowered strength. We study the case where specimens that have transverse failure strains lower than two standard deviations below the mean are rejected (2.3% rejection rate). We construct three new DRS for PSF corresponding to error bounds of 0, 10%, and 20%.

The probabilistic design optimizations of composite laminates for three different values of error bound (b_e) are performed and the results are presented in Table 7 and in Fig. 4. We note that when this form of variability reduction is applied, the laminate

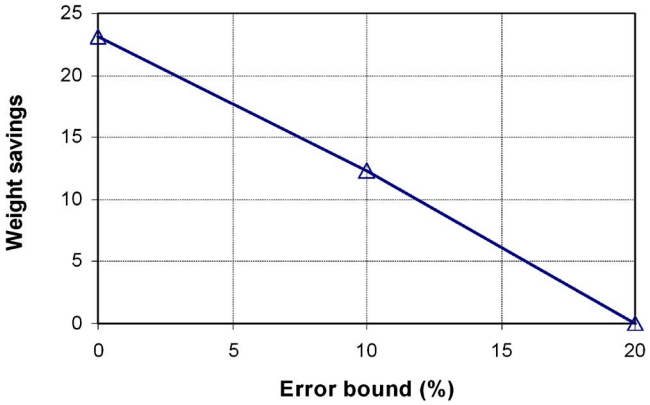

Fig. 3 Reducing laminate thickness (hence weight) by error reduction (no variability reduction)

Table 7 Probabilistic optimum designs for different error bounds when both error and variability reduction are applied. PSF and P_f given in the last two columns are calculated via MCS (sample size of 10,000,000) where the strains are directly computed via the standard CLT analysis. The numbers in parentheses under PSF and P_f show the standard errors due to limited sample size of MCS.

Error bound	θ_1 θ_2 (deg)	t_1 t_2 (in.)	h (in.) $[\Delta h(\%)]$[a]	PSF	P_f ($\times 10^{-4}$)
0	28.52	0.0089	0.0813	0.9965	1.255
	28.71	0.0114	[−46.6]	(0.0014)	(0.035)
10%	27.34	0.0129	0.0970	1.0016	0.906
	27.37	0.0144	[−36.2]	(0.0015)	(0.030)
20%	25.57	0.0168	0.1224	0.9968	1.190
	25.66	0.0138	[−19.5]	(0.0015)	(0.109)

[a]The optimum laminate thickness for the 20% error bound given in Table 6 (i.e. $h=0.1520$ in.) is taken as the basis for Δh computations.

thickness can be reduced by 19.5%. If the error bound is reduced from 20% to 10% together with the variability reduction, the laminate thickness can be reduced by 36.2%.

The numbers in the last two columns of Table 7 show the PSF and P_f calculated by using the 10,000,000 MCS where strains are directly calculated through the standard CLT analysis. The design values for PSF and P_f of the optimum designs are expected to be 1.0 and 10^{-4}. Discrepancies can be the result of the following.

1. Error due to the use of normal distributions for strains which may not exactly follow normal distributions;
2. Error due to limited sample size of MCS while calculating the mean and standard distribution of strains;
3. Error due to limited sample size of MCS while computing the probabilistic sufficiency factor PSF; and
4. Error associated with the use of response surface approximations for PSF.
5. Error due to neglecting correlations between strains.

Next, a plot for the probability of failure (calculated via 1,000,000 MCS), weight and error reduction measures is shown in Fig. 5. The optimum ply angles for the case with 20% error bound and no variability reduction are 25.59 deg and 25.53 deg. Here we take both ply angles at 25 deg. We note from Fig. 5 that for our problem, the error reduction is a more effective way of reducing weight compared to the specified variability reduction when the target probability of failure of the laminates is higher than 2×10^{-4} and quality control is more effective for lower probabilities.

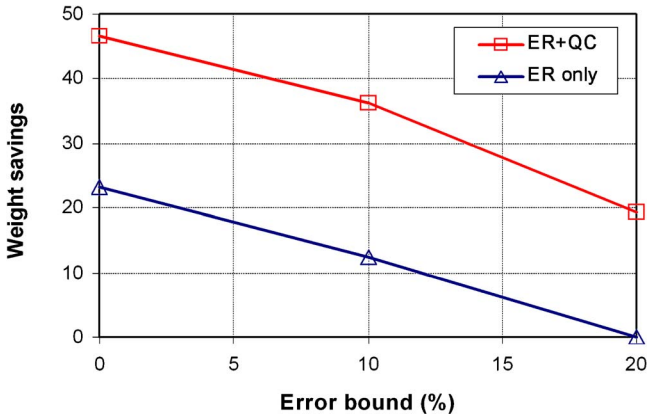

Fig. 4 Reducing laminate thickness by error reduction (ER) and quality control (QC)

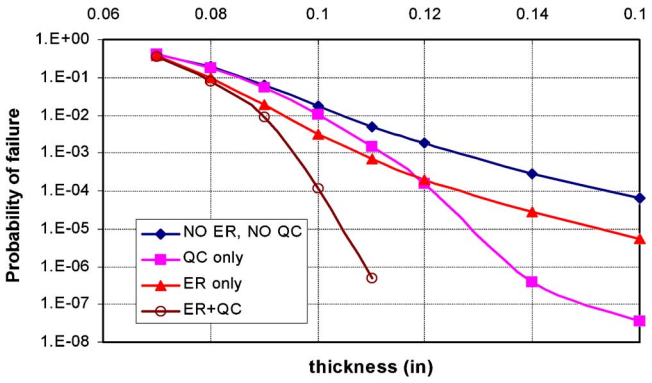

Fig. 5 Tradeoff plot for the probability of failure, design thickness, and uncertainty reduction measures: (ER) error reduction (reducing from 20% to 10%), (QC) quality control to -2σ

6 Choosing Optimal Uncertainty Reduction Combination

Obviously, when it comes to a decision of what uncertainty reduction mechanisms to use, the choice depends on the cost of the uncertainty reduction measures. For a company, the costs of small error reduction may be moderate, since they may involve only a search of the literature for the best models available. Substantial error reduction may entail the high cost of doing additional research. Similarly, small improvements in variability, such as improved quality control may entail using readily available nondestructive testing methods, while large improvements may entail developing new methods, or acquiring expensive new equipment. To illustrate this, we assume a hypothetical cost function in quadratic form

$$\text{cost} = A(\text{ER})^2 + B(\text{QC}+3)^2 \tag{8}$$

where A and B are cost parameters, ER represents the error reduction, and QC stands for the number of standard deviations that are the threshold achieved by quality control. We generated hypothetical cost contours by using Eq. (8) as shown in Fig. 6. The nominal value of error is taken as 20% and we assume that the quality control to -3σ is associated with no cost. For example, if error is reduced from 20% to 15%, ER=0.20−0.15=0.05. Similarly, if quality control to -2.5σ is employed, then QC+3 takes the value of 0.5. As an example we take $A=\$20$ million and $B=\$100{,}000$.

Next, we generated tradeoff plot for probability of failure and uncertainty reduction measures for laminates of thickness $t_1=0.010$ in. and $t_2=0.015$ in. as shown in Fig. 6. The optimum ply angles are calculated such that they minimize the probability of failure. The probabilities of failure are calculated via MCS (sample size of 10^6). The hypothetical cost contours for the uncertainty reduction measures given in Fig. 6 enable a designer to identify the optimal uncertainty control selection. We see in Fig. 6 that for high probabilities quality control is not cost effective, while for low failure probabilities quality control becomes more effective and a proper combination of error reduction and quality control leads to a minimum cost.

7 Concluding Remarks

The tradeoffs of uncertainty reduction measures for minimizing structural weight were investigated. Inspired by the allocation of the risk between the components of a system for minimal cost, the optimal allocation of uncertainty as error and variability was analyzed. As a demonstration problem, the design of composite laminates at cryogenic temperatures was chosen because the design is very sensitive to uncertainties. Quality control was used as a way to reduce variability, and its effect was compared to the effect of reducing error in the analysis. Tradeoff plots of uncertainty reduction measures, probability of failure and weight were generated

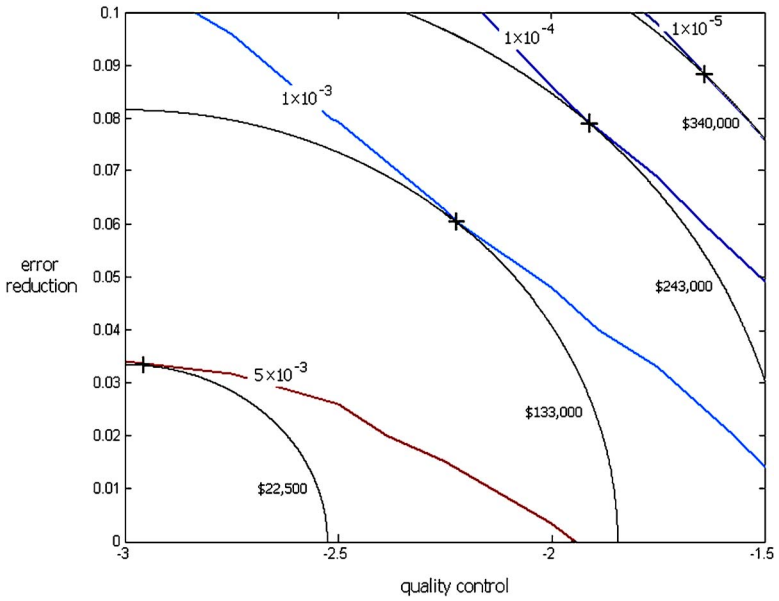

Fig. 6 Tradeoff of probability of failure and uncertainty reduction. Probabilities of failure are calculated via MCS (sample size of 1,000,000). The crosses in the figure indicate the optimal uncertainty control combination that minimizes the cost of uncertainty control for a specified probability of failure.

that would enable a designer to choose the optimal uncertainty control measure combination to reach a target probability of failure with minimum cost.

For this specific example problem we observed the following:

1. Reducing errors from 20% to 10% led to 12% weight reduction;
2. Quality control to $-2\ \sigma$ led to 20% weight reduction;
3. The use combined of error reduction and quality control mechanisms reduced the weight by 36%; and
4. Quality control was more effective at low required failure probabilities, while the opposite applied for higher required probabilities of failure.

In addition, a computational procedure for estimating the probability of failure based on approximating the cumulative distribution functions for strains in a conservative manner was developed. We found that this approach led to more accurate probability of failure estimates than response surface approximations of the response.

Acknowledgment

This work has been supported in part by the NASA Constellation University Institute Program (CUIP), Ms. Claudia Meyer program monitor, and NASA Langley Research Center Grant No. NAG1-03070, Dr. W. J. Stroud program monitor.

Appendix A. Temperature Dependent material Properties

Since we analyze the problem that was addressed by Qu et al. [19], the geometry, material parameters and the loading conditions are taken from that paper. Qu et al. [19] obtained the temperature dependent properties by using the material properties of IM600/133 given in Aoki et al. [26] and fitted with smooth polynomials in order to be used in calculations. The reader is referred to Appendix A of Qu et al. [19] for the details. The temperature dependent material properties are shown in Figs. 7 and 8.

Appendix B. Details of Conservative Cumulative Distribution Function (CDF) Fitting

As we noted earlier, we assume normal distributions for strains and estimate the mean and the standard deviation of the assumed distributions conservatively. Conservative fitting is assessed as follows. We first perform Monte Carlo simulations with sample size of 1000 and calculate the mean and the standard deviation of the strains. Then we assume that the strains follow normal distribution with the calculated mean and standard deviation. We see in Fig. 2(*a*) that the normal CDF is smaller than the empirical CDF for some strain values, and larger for other strain values. That is, the normal CDF leads to conservative estimates for some strain values, while it leads to unconservative estimates for other strain values. It is desirable to have conservative estimates for all strain values, that is, to have a conservative CDF fit which is smaller than the empirical CDF for all strain values. However, the tails of the distribution are volatile, and fitting conservative CDF including these values can lead to over conservative results. Accord-

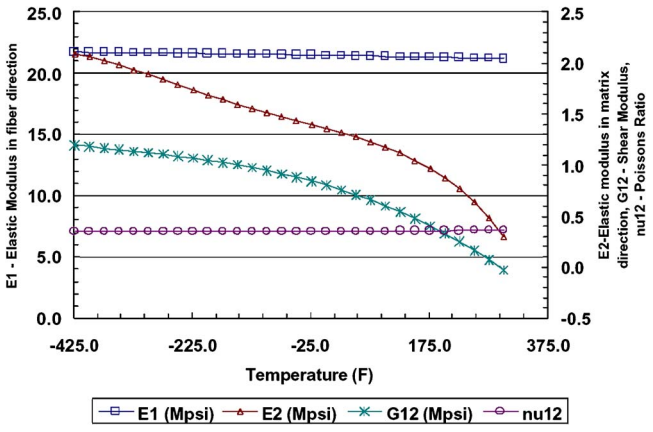

Fig. 7 Material properties E_1, E_2, G_{12}, and ν_{12} as a function of temperature

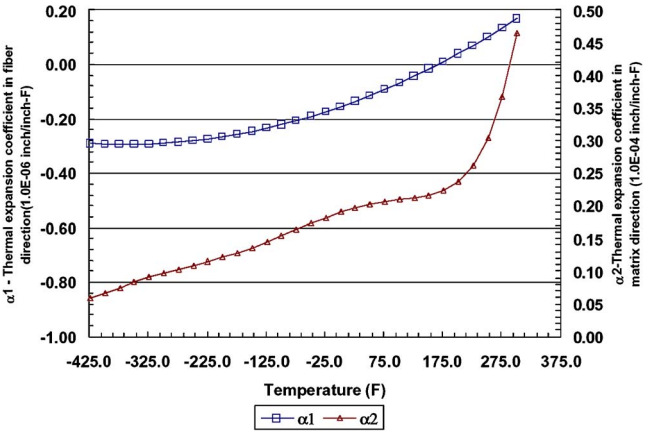

Fig. 8 Material properties α_1 and α_2 as a function of temperature

ingly, we do not apply constraints to the first five points (out of 1000 points) of the left tail and last five points of the right tail. Out of the remaining 990 points, we choose uniformly spaced 100 points and calculate the maximum deviation of the normal CDF fit from the empirical CDF fit at these 100 points. The maximum deviation of the fitted CDF for the empirical CDF is called the Kolmogorov–Smirnov distance. We shift the mean value of the fitted CDF to close the Kolmogorov–Smirnov distance between the normal fit and empirical fit. The normal distribution with this shifted mean and original standard deviation is our conservative normal fit. As we see in Fig. 2(*a*) that the conservative normal CDF lies below the empirical CDF for all strains except near the tails.

A better conservative fit can possibly be obtained by varying the mean and standard deviation at the same time. Detailed investigation on conservative estimation of CDF for probability of failure calculations is provided in Picheny et al. [27].

Appendix C. Details of Design Response Surface Fitting

Qu et al. [19] showed that using the combination of face centered central composite design (FCCCD) and Latin hypercube sampling (LHS) designs gives accurate results, so we follow the same procedure.

The ranges for design variables for DRS are decided as follows. The initial estimates of the ranges for design variables were taken from Qu et al. [19]. When we used these ranges, we found that the prediction variances at the optimum designs were unacceptably large. The ranges for DRS were then reduced by zooming around the optimum designs obtained from the wider ranges. After zooming, the prediction variances at the optimum designs were found to be smaller than the RMSE predictors. The final ranges for response surfaces are given in Table 8.

Table 8 The ranges of variables for the three DRS constructed for P_f calculation

	t_1 and t_2 (in.)	θ_1 and θ_2 (deg)
$b_e=0$	0.012–0.017	24–27
$b_e=10\%$	0.013–0.018	24–26
$b_e=20\%$	0.015–0.022	22–25

Qu et al. [19] used a fifth-order DRS for the probability of failure, and found it to be quite accurate. We also use a fifth-order DRS. A fifth-order response surface in terms of four variables has 126 coefficients. Following Qu et al. [19], we used 277 design points, 25 correspond to FCCCD and 252 are generated by LHS. In addition to response surfaces for probability sufficiency factor, three more DRS were also fitted to the probability of failure for comparison purpose. The comparison of the accuracies of DRS for PSF and DRS for P_f are shown in Table 9. For instance, for error bound of 20%, the root mean square error predictions of DRS for PSF and DRS for P_f are 3.610×10^{-3} and 7.664×10^{-4}, respectively. Since PSF and P_f are not of the same order of magnitude, we cannot compare these errors directly. One possibility is to compare the ratios of RMSE and mean of the response. When we compare the ratios for error bound of 20%, we see that the ratio of RMSE and mean of the response DRS for P_f is 0.1868, while the same ratio of DRS for PSF is 0.0042. It is an indication that DRS for PSF is more accurate than DRS for P_f.

Another way of comparing the accuracies is to calculate equivalent errors of DRS for PSF to those of DRS for P_f. That is, the equivalent error in P_f due to error in DRS for PSF can be compared to the equivalent error in PSF due to error in DRS for P_f.

The standard errors in calculation of PSF and P_f due to limited MCS sample size are given in the last two columns of Table 6. The standard error for P_f is calculated from

$$\sigma_P = \sqrt{\frac{P_f(1-P_f)}{N}} \tag{C1}$$

The standard error in PSF is calculated as illustrated in the following example. Assume that for calculating a probability of

Table 9 Accuracies of DRS fitted to PSF and P_f in terms of four design variables (t_1, t_2, θ_1 and θ_2) for error bounds, b_e, of 0, 10%, and 20%

		Mean of response	RMSE predictor	Ratio of RMSE to the mean of response	Equivalent error in P_f	Equivalent error in PSF
$b_e=0\%$	PSF	1.077	4.655×10^{-3}	4.332×10^{-3}	5.397×10^{-7} ($<9.447\times10^{-4}$)	—
	P_f	8.081×10^{-4}	9.447×10^{-4}	1.196	—	4.205×10^{-2} ($>4.655\times10^{-3}$)
$b_e=10\%$	PSF	0.9694	4.645×10^{-3}	4.792×10^{-3}	4.615×10^{-6} ($<8.281\times10^{-4}$)	—
	P_f	1.340×10^{-3}	8.281×10^{-4}	0.6180	—	1.862×10^{-2} ($>4.645\times10^{-3}$)
$b_e=20\%$	PSF	0.8621	3.610×10^{-3}	4.187×10^{-3}	6.308×10^{-5} ($<7.664\times10^{-4}$)	—
	P_f	4.103×10^{-3}	7.664×10^{-4}	0.1868	—	1.013×10^{-2} ($>3.610\times10^{-3}$)

Table 10 Ranges of design variables for the three DRS constructed for probability of failure estimation for the error and variability reduction case

	t_1 and t_2 (in.)	θ_1 and θ_2 (deg)
$b_e=0$	0.008–0.012	27–30
$b_e=10\%$	0.009–0.014	26–29
$b_e=20\%$	0.013–0.018	24–27

failure of 1×10^{-4}, we use sample size of 10^6 in MCS. Then, the number of simulations failed is 100 and the standard error for P_f calculation from Eq. (C1) is 1×10^{-5}. Thus, ten simulations out of 100 represent the standard error. The standard error in PSF can be approximated as the difference between the 105th smallest safety factor and 95th smallest safety factor. A better estimation for PSF can be obtained by utilizing the CDF of the safety factor S.

The equivalent error in P_f due to the error in DRS for PSF, for error bound of 20% for instance, can be approximated as follows. The mean of response and RMSE prediction of DRS for PSF are $\mu=0.8621$ and $\sigma=3.610\times10^{-3}$, respectively. We calculate the P_f values corresponding to PSF values of μ-$\sigma/2$ and μ-$\sigma/2$ as 4.605×10^{-4} and 3.974×10^{-4}, respectively. The difference between these two P_f values, 6.31×10^{-5}, gives an approximation for the equivalent error in P_f. We see that this equivalent error in P_f is smaller than the error in DRS for P_f, 7.664×10^{-4}, indicating that the DRS for PSF has better accuracy than DRS for P_f. The equivalent error in PSF due to errors in DRS for P_f can be computed in a similar manner. The equivalent error in PSF (1.013×10^{-2}) due to error in DRS for P_f is larger than the error in DRS for PSF (3.610×10^{-3}) indicating that the DRS for P_f does not have good accuracy. The errors in DRS for P_f are clearly unacceptable in view that the required probability of failure is 1×10^{-4}.

DRS for Error Reduction and Quality Control Case. Table 8 showed the ranges of design variables for DRS when only error reduction was of interest. When quality control is also considered, we changed the ranges of the design variables. All properties such as the design of experiments and the degree of polynomial were kept the same for the new response surfaces; the only change made was the ranges of design variables. The new ranges of design variables used while constructing the new response surfaces are given in Table 10. Notice that the ranges for laminates thicknesses are reduced and ranges for ply angles are increased, the safety of the laminates are further improved by addition of quality control.

Nomenclature

α_1, α_2 = coefficient of thermal expansion along and transverse to fiber direction
b_e = bound of error
Δh = weight saving (i.e., thickness reduction)
ε_1, ε_2, γ_{12} = strains in the fiber direction, transverse to the fiber direction, and shear strain of a composite ply, respectively.
E_1, E_2, G_{12} = elastic modulus along and transverse to fiber direction and shear modulus of a composite ply, respectively.
h = total laminate thickness
ν_{12} = major Poisson's ratio of a composite ply
N_x and N_y = mechanical loading in x and y directions, respectively
P_f and PSF = probability of failure and probability sufficiency factor, respectively
R^2_{adj} = adjusted coefficient of multiple determination
RMSE = root mean square error
S_F = safety factor
θ, θ_1, θ_2 = ply orientation angles
t_1, t_2 = thickness of plies with angles θ_1 and θ_2, respectively
T_{zero} = stress free temperature
T_{serv} = service temperature

Superscripts

U = upper limit
L = lower limit

References

[1] Mohamed, A., Lawrence, L. M., and Ravindran, A., 1991, "Optimization Techniques for System Reliability: A Review," Reliab. Eng. Syst. Saf., **35**(2), pp. 137–146.
[2] Knoll, A., 1983, "Component Cost and Reliability Importance for Complex System Optimization," *Proceedings of the International ANS/ENS Topical Meeting on Probabilistic Risk Assessment*, Vol. 11, Port Chester, N.Y., September.
[3] Hurd, D. E., 1980, "Risk Analysis Methods Development," General Electric Report No. GEFR-14023–13, April–June.
[4] Gokcek, O., Temme, M. I., and Derby, S. L., 1978, "Risk Allocation Approach to Reactor Safety Design and Evaluation," *Proceedings of the Topical Meeting on Probabilistic Analysis of Nuclear Reactor Safety*, Los Angeles, CA, May 8.
[5] Cho, N. Z., Papazoglou, I. A., and Bari, R. A., 1986, "A Methodology for Allocating Reliability and Risk," Report No. NUREG/CR-4048, Brookhaven National Laboratory, Upton, NY.
[6] Yang, X. P., Kastenberg, W. E., and Okrent, D., 1989, "Optimal Safety Goal Allocation for Nuclear Power Plants," Reliab. Eng. Syst. Saf., **25**(3), pp. 257–278.
[7] Yang, J., Hwang, M., Sung, T., and Jin, Y., 1999, "Application of Genetic Algorithm for Reliability Allocation in Nuclear Power Plants," Reliab. Eng. Syst. Saf., **65**, pp. 229–238.
[8] Ivanovic, G., 2000, "The Reliability Allocation Application in Vehicle Design," Int. J. Veh. Des., **24**(2–3), pp. 274–286.
[9] Acar, E., and Haftka, R. T., 2005, "Reliability Based Aircraft Structural Design Optimization with Uncertainty About Probability Distributions," *Proceedings of the 6th World Congress on Structural and Multidisciplinary Optimization*, Rio de Janeiro, Brazil, 30 May–3 June 2005.
[10] Vogler, K-H., 1997, "Risk Allocation and Inter-Dealer Trading," Eur. Economic Rev., **41**(8), pp. 1615–1634.
[11] Bing, L., Akintoye, A., Edwards, P. J., and Hardcastle, C., 2005, "The Allocation of Risk in PPP/PFI Construction Projects in the UK," Int. J. Proj. Manage. **23**(1), pp. 25–35.
[12] Niehaus, G., 2002, "The Allocation of Catastrophe Risk," J. Bank. Finance, **26**(2–3), pp. 585–596.
[13] Oberkampf, W. L., DeLand, S. M., Rutherford, B. M., Diegert, K. V., and Alvin, K. F., 1999, "A New Methodology for the Estimation of Total Uncertainty in Computational Simulation," *Proceedings of the AIAA Non-Deterministic Approaches Forum*, St. Louis, MO, April, AIAA Paper No. 99–1612.
[14] Oberkampf, W. L., Deland, S. M., Rutherford, B. M., Diegert, K. V., and Alvin, K. F., 2002, "Error and Uncertainty in Modeling and Simulation," Reliab. Eng. Syst. Saf. **75**, pp. 333–357.
[15] Acar, E., Kale, A., Haftka, R. T., and Stroud, W. J., 2006, "Structural Safety Measures for Airplanes," J. Aircr. **43**(1), pp. 30–38.
[16] Acar, E., Kale, A., and Haftka, R. T., 2007, "Comparing Effectiveness of Measures that Improve Aircraft Structural Safety," ASCE Journal of Aerospace Engineering, to be published.
[17] Acar, E., Haftka, R. T., Sankar, B. V., and Qui, X., 2006, "Increasing Allowable Flight Loads by Improved Structural Modeling," AIAA J. **44**(2), pp. 376–381.
[18] Kale, A., Haftka, R. T., and Sankar, B. V., 2005, "Reliability Based Design and Inspection of Stiffened Panels Against Fatigue," *Proceedings of the 46th AIAA/ASME/ASCE/AHS/ASC Structures, Structural Dynamics & Materials Conference*, Austin, TX, AIAA Paper No. 2005–2145.
[19] Qu, X., Haftka, R. T., Venkataraman, S., and Johnson, T. F., 2003, "Deterministic and Reliability-Based Optimization of Composite Laminates for Cryogenic Environments," AIAA J. **41**(10), pp. 2029–2036.
[20] Antonsson, E. K., and Otto, K. N., 1995, "Imprecision in Engineering Design," ASME J. Mech. Des. **117** pp. 25–32.
[21] Nikolaidis, E., Chen, S., Cudney, H., Haftka, R. T., and Rosca, R., 2004, "Comparison of Probability and Possibility for Design Against Catastrophic Failure Under Uncertainty," ASME J. Mech. Des. **126**, pp. 386–394.
[22] Vanegas, L. V., and Labib, A. W., 2005, "Fuzzy Approaches to Evaluation in Engineering Design," ASME J. Mech. Des. **127**, pp. 24–33.
[23] Ifju, P. G., Niu, X., Kilday, B. C., Liu, S. C., and Ettinger, S. M., 2000, "Residual Strain Measurement in Composites Using the Cure-Referencing Method," Exp. Mech. **40**(1), pp. 22–30.
[24] Qu, X., and Haftka, R. T., 2004, "Reliability-Based Design Optimization Using Probabilistic Sufficiency Factor," Struct. Multidiscip. Optim. **27**(15), pp. 314–325.

[25] Schultz, W., Smarslok, B., Speriatu, L., Ifju, P. G., and Haftka, R. T., 2005, "Residual Stress Determination Using Temperature Dependent Material Properties and Uncertainty Analysis," *Proceedings of the SEM Annual Conference and Exposition*, Portland, OR, June 7–9.
[26] Aoki, T., Ishikawa, T., Kumazawa, H., and Morino, Y., 2000, "Mechanical Performance of CF/Polymer Composite Laminates Under Cryogenic Conditions," *Proceedings of the 41st AIAA/ASME/ASCE/AHS/ASC Structures, Structural Dynamics, and Materials Conference*, Atlanta, GA, April 3–6, AIAA Paper No. 2000–1605.
[27] Picheny, V., Kim, N. H, and Haftka, R. T., 2006, "Conservative Estimation of Probability of Failure," *Proceedings of the 11th AIAA/ISSMO Multidisciplinary Analysis and Optimization Conference*, Portsmouth, VA, September 6–8.